Обзор ArXiv/astro-ph, 26-30 октября 2020

От Сильченко О.К.

ArXiv:2010.13845

Disk dominated galaxies retain their shapes below $z = 1.0$

K. Hoffmann[1⋆], C. Laigle[2], N. E. Chisari[3], P. Tallada[4,5], Y. Dubois[2], J. Devriendt[6]

[1] *Institute for Computational Science, University of Zurich, Winterthurerstr. 190, 8057 Zürich, Switzerland*
[2] *CNRS and UPMC Univ. Paris 06, UMR 7095, Institut d'Astrophysique de Paris, 98 bis Boulevard Arago, F-75014 Paris, France*
[3] *Institute for Theoretical Physics, Utrecht University, Princetonplein 5, 3584 CC Utrecht, The Netherlands*
[4] *Centro de Investigaciones Energéticas, Medioambientales y Tecnológicas (CIEMAT), Avenida Complutense 40, 28040 Madrid, Spain*
[5] *Port d'Informació Científica (PIC), Campus UAB, C. Albareda s/n, 08193 Bellaterra (Barcelona), Spain*
[6] *Astrophysics, University of Oxford, Denys Wilkinson Building, Keble Road, Oxford, OX1 3RH, UK*

Accepted XXX. Received YYY; in original form ZZZ

ABSTRACT

The high abundance of disk galaxies without a large central bulge challenges predictions of current hydrodynamic simulations of galaxy formation. We aim to shed light on the formation of these objects by studying the redshift and mass dependence of their 3D shape distribution in the COSMOS galaxy survey. This distribution is inferred from the observed distribution of 2D shapes, using a reconstruction method which we test using hydrodynamic simulations. We find a moderate bias for the inferred average disk circularity and relative thickness with respect to the disk radius, but a large bias on the dispersion of these quantities. Applying the 3D shape reconstruction method on COSMOS data, we find no significant dependence of the inferred 3D shape distribution on redshift. The relative disk thickness shows a significant mass dependence which can be accounted for by the scaling of disk radius with galaxy mass.

Обзор COSMOS

- 2 квадратных градуса.
- 30 фотометрических полос от 0.2 мкм до 24 мкм (Subaru, VISTA, CFHT, Spitzer…) → красные смещения, звездные массы, темпы SF по SED (252 тыс. галактик).
- Изображения с HST/ACS →FWHM*=0.085”→GALFIT → отношение осей (128 тыс. галактик).
- ZEST – морфологическая классификация – disk-dominated galaxies (109 тыс. галактик).
- После пересечения всех каталогов – volume-limited sample 3739 галактик.

Окончательные отсечки

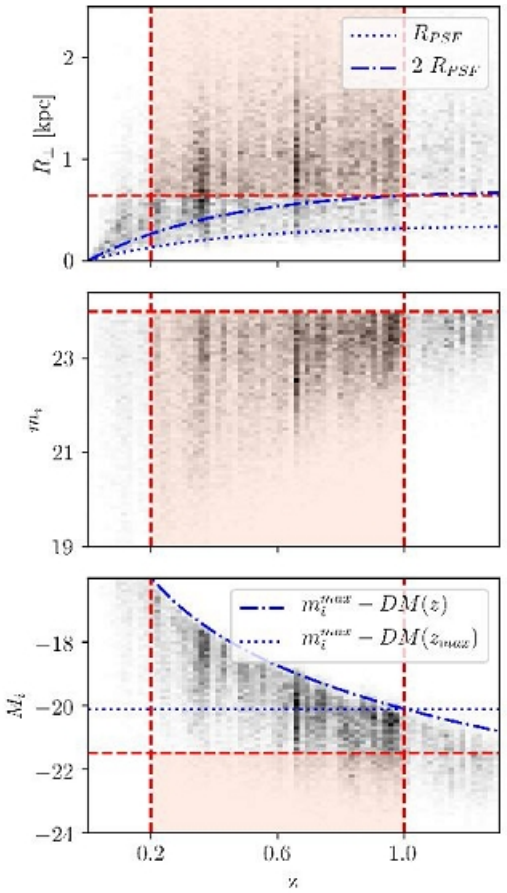

Figure 2. Selection of the volume limited main sample from disk dominated galaxies in the matched COSMOS catalogue by photometric redshift z, transverse comoving radii $R_\perp$ and apparent and absolute i band magnitudes m_i and M_i respectively. The cuts on each variable are marked by red dashed lines, enclosing the selected sample in the red area. The blue dotted and dashed-dotted lines in the top panel show the comoving radii which correspond to one and two times the angular size of the HST PSF respectively. The blue dashed-dotted line in the bottom panel shows the limit on M_i, given

galaxy property	constraint
photometric redshift	$0.2 < z < 1.0$
apparent 3″ aperture AB Subaru i+ magnitude	$m_i < 24$
absolute rest-frame Subaru i+ magnitude	$M_i < -21.5$
transverse comoving effective radius	$R_\perp > 0.64$ kpc

Table 1. Selection cuts for the volume limited COSMOS main sample, shown in Fig. 2

Примеры изображений с HST

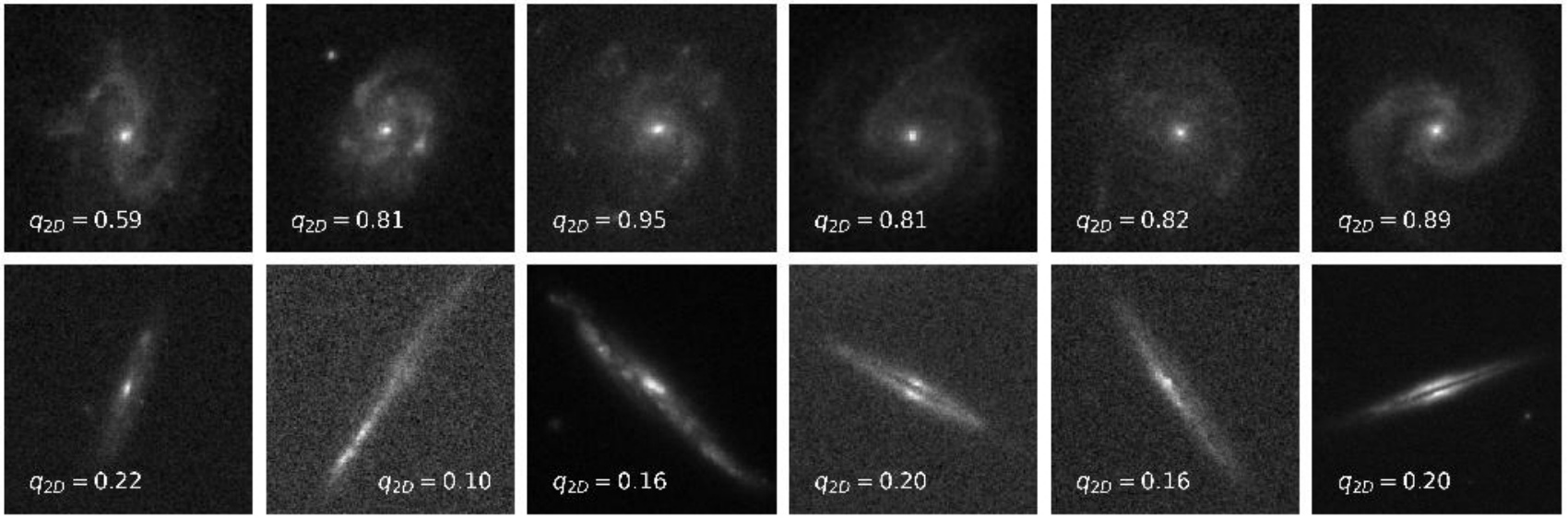

Figure 1. Examples of ACS images of late type galaxies in our volume limited COSMOS sample in the redshift range $0.2 < z < 0.4$ with face-on and edge-on orientations (top and bottom panels respectively). The galaxies are selected to be disk-dominated according to the ZEST morphological classification scheme (Section 2.1.3). The 2D axes ratios q_{2D}, provided in the ACS-GC catalogue, where obtained from single Sérsic profile fits (Section 2.1.2). The image sizes are adjusted for each galaxy.

Статистика типов в обзоре COSMOS - традиционная

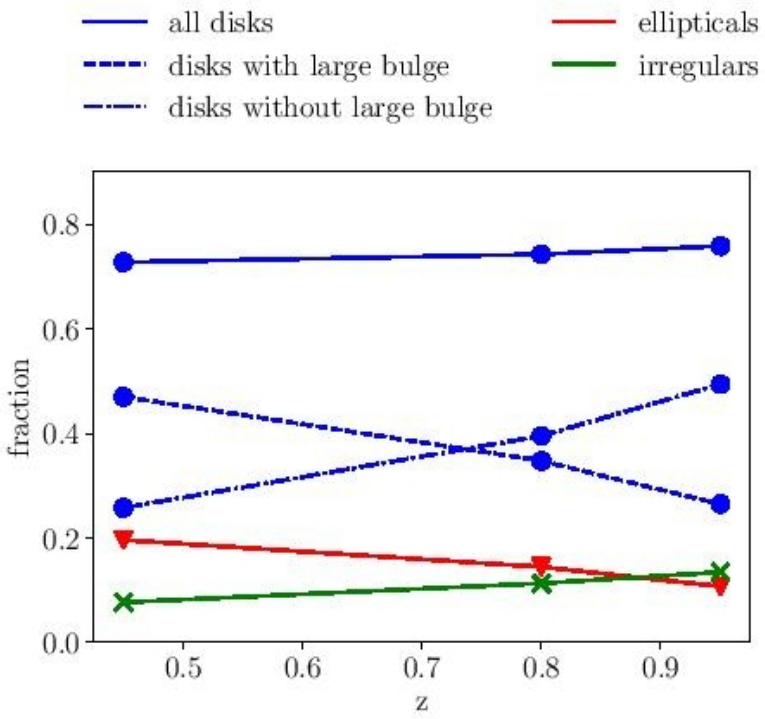

Figure 5. Fractions of galaxy types in our volume limited COSMOS sample in the three redshifts bins shown in Fig. 7. Blue circles, red triangles and green crosses show results for galaxies classified as disks, ellipticals and irregulars respectively. Results for disks with and without a large bulge are connected by dashed-dotted and dashed lines respectively.

Эволюция?

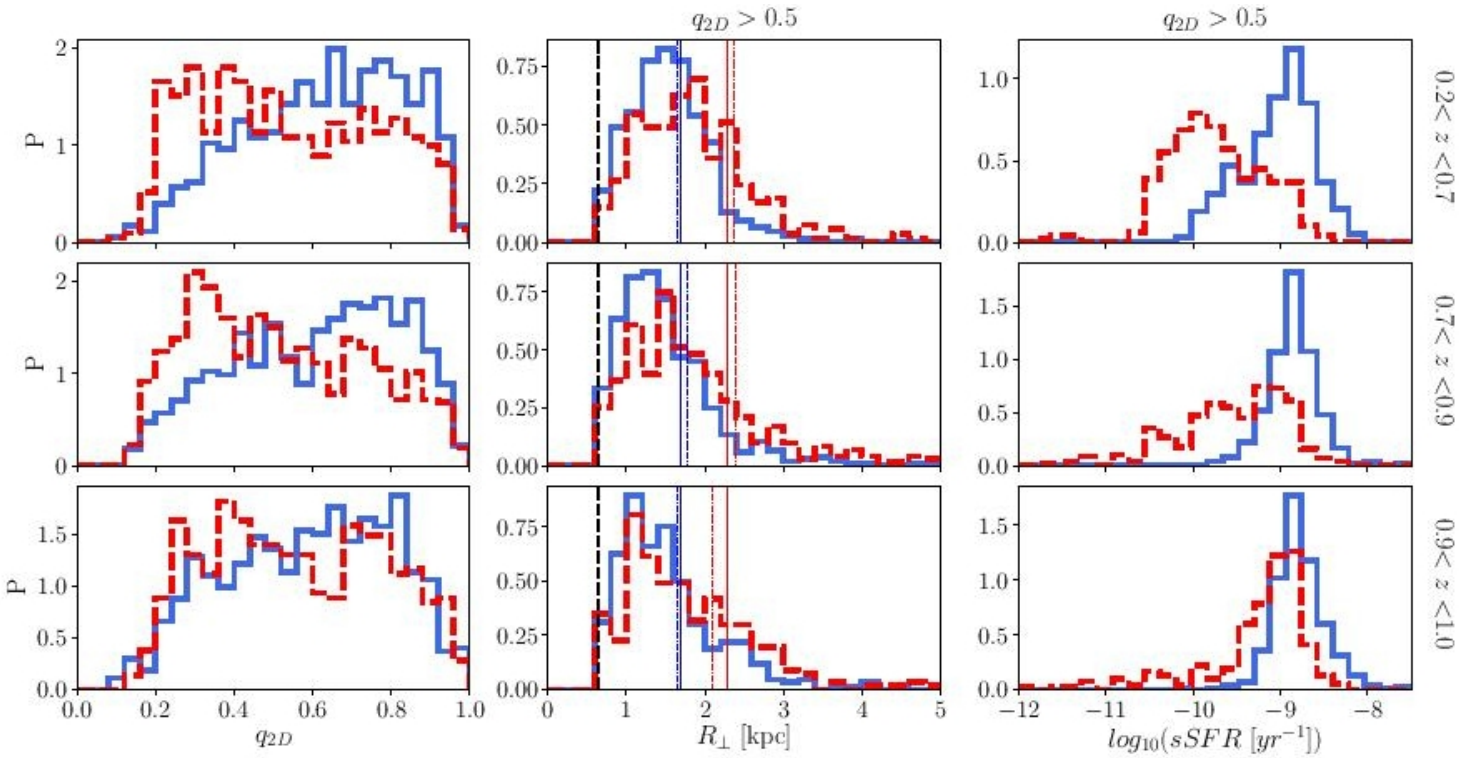

Figure 9. Probability distributions of apparent 2D axes ratios, transverse comoving radii and specific star formation rates (left, central and right panels respectively) for disk dominated galaxies in our volume limited COSMOS main sample with stellar masses below and above $10^{10.35}M_\odot$ (blue and red histograms respectively). Vertical panels show results in three redshift bins with limits indicated on the right. The comoving radii and specific star formation rates are shown for disks with apparent axes ratios above $q_{2D} > 0.5$, to minimize bias induced by projection and dust extinction (see Fig. 4 and B1). Vertical black dashed lines mark the minimum radius of the volume limited sample. Vertical solid and dotted lines indicate the mean radii for each mass sample over the full redshift range and in each redshift bin respectively.

Сравнения с формами галактик в космологических симуляциях

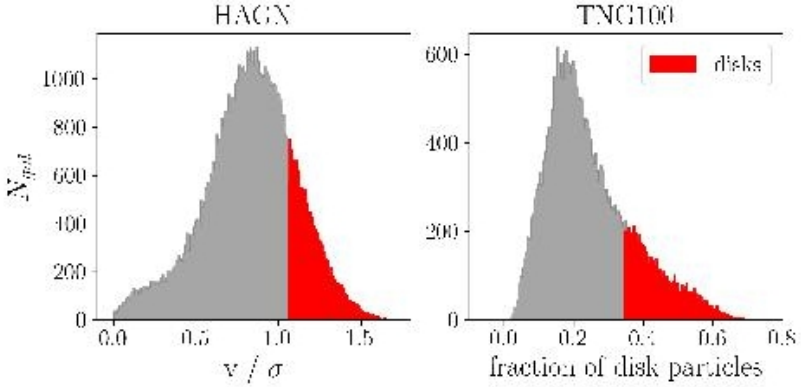

Figure 10. *Left*: Distribution of the ratio between stellar rotation $V_{\rm rot}$ and the velocity dispersion σ_v for galaxies in the HAGN simulation. *Right*: Distribution of the fraction of disk particles in each galaxy of the TNG100 simulations. The populations of galaxies which we classify as disks are marked in red at the tails of the distributions, and make up 20 % of the entire sample. Results are shown for $z = 1.0$.

		TNG100	HAGN
Ω_Λ	-	0.6911	0.728
Ω_m	-	0.3089	0.272
Ω_b	-	0.0486	0.045
H_0	$[s^{-1}km]$	67.74	70.4
σ_8	-	0.8159	0.81
n_s	-	0.9667	0.967
$L_{\rm box}$	$[h^{-1}Mpc]$	75	100
$m_\star$	$[M_\odot]$	-	2×10^6
$m_{\rm baryon}$	$[M_\odot]$	1.4×10^6	-
$m_{\rm dm}$	$[M_\odot]$	7.5×10^6	8×10^7

Table 2. Main properties of the hydro-dynamic simulations Illustris TNG 100 and Horizon AGN.

Выбор дисков!

Это в результате 2D и 3D формы у модельных дисковых галактик

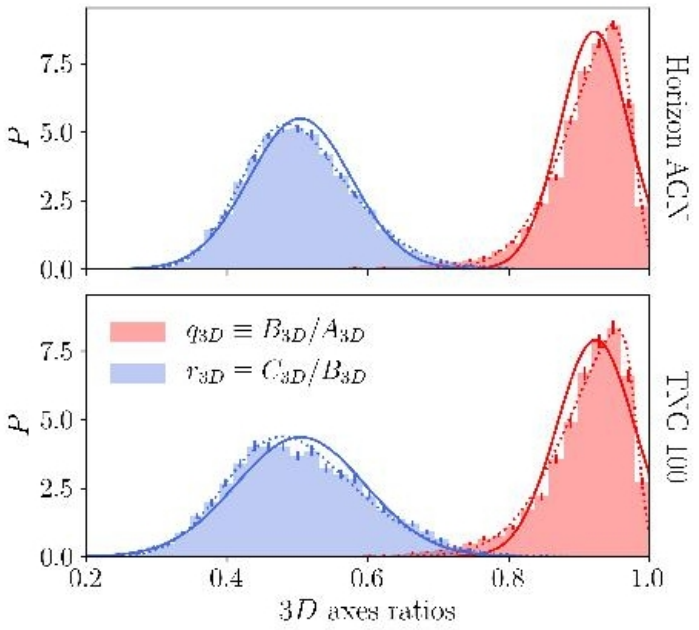

Figure 11. Distributions of 3D axes ratios for disk galaxies in hydrodynamic simulations at $z = 1.0$, obtained from the simple moment of inertia. Solid and dotted lines show fits to a normal and a skew normal distribution respectively.

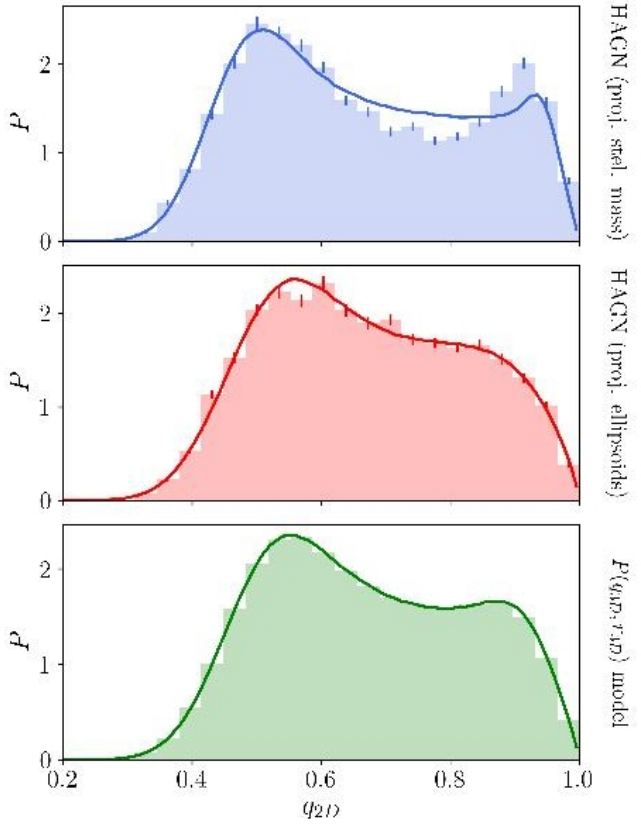

А это результат для реальных галактик из обзора COSMOS

stellar mass range	redshift range	N_{gal}	q_0	σ_q	r_0	σ_r	s_0	$\chi^2/d.o.f.$
$M_\star < 10^{10.35} M_\odot$	$0.2 < z < 1.0$	1913	$0.873^{0.895}_{0.864}$	$0.072^{0.1}_{0.06}$	$0.37^{0.385}_{0.357}$	$0.207^{0.232}_{0.195}$	$0.325^{0.339}_{0.314}$	1.282
	$0.2 < z < 0.7$	441	$0.889^{0.911}_{0.819}$	$0.051^{0.224}_{0.039}$	$0.427^{0.631}_{0.407}$	$0.207^{0.286}_{0.184}$	$0.377^{0.526}_{0.362}$	0.577
	$0.7 < z < 0.9$	785	$0.86^{0.884}_{0.841}$	$0.073^{0.114}_{0.056}$	$0.276^{0.314}_{0.112}$	$0.348^{0.522}_{0.295}$	$0.234^{0.273}_{0.095}$	0.982
	$0.9 < z < 1.0$	681	$0.833^{0.864}_{0.8}$	$0.064^{0.213}_{0.051}$	$0.353^{0.464}_{0.331}$	$0.201^{0.287}_{0.178}$	$0.295^{0.395}_{0.278}$	1.134
$M_\star > 10^{10.35} M_\odot$	$0.2 < z < 1.0$	1836	$0.906^{0.973}_{0.888}$	$0.147^{0.18}_{0.116}$	$0.257^{0.265}_{0.25}$	$0.055^{0.06}_{0.05}$	$0.24^{0.252}_{0.227}$	1.388
	$0.2 < z < 0.7$	530	$0.88^{0.939}_{0.862}$	$0.072^{0.148}_{0.055}$	$0.244^{0.257}_{0.235}$	$0.042^{0.055}_{0.032}$	$0.214^{0.234}_{0.208}$	0.793
	$0.7 < z < 0.9$	766	$0.983^{0.979}_{0.88}$	$0.254^{0.292}_{0.206}$	$0.271^{0.29}_{0.259}$	$0.055^{0.068}_{0.042}$	$0.256^{0.275}_{0.236}$	1.175
	$0.9 < z < 1.0$	536	$0.919^{0.972}_{0.882}$	$0.119^{0.154}_{0.082}$	$0.281^{0.298}_{0.268}$	$0.088^{0.105}_{0.072}$	$0.259^{0.28}_{0.245}$	0.874

Table 4. Parameters of model for the 3D axes ratio distribution (equation (5) and (6)), inferred from fits to the 2D axis ratio distribution, shown in Fig. 15. Results are shown for the six redshift-stellar mass samples and two mass samples defined over the full redshift range, as indicated in the left columns. For each model parameter we provide the lower and upper limit of the 68% confidence level, obtained from the marginalized posteriors. The distributions of the 3D axis ratios, predicted for COSMOS based on these parameters, are shown in Fig. 17.

r - относительная толщина дисков

q - отношение осей в экваториальной плоскости

А есть ли эволюция форм?

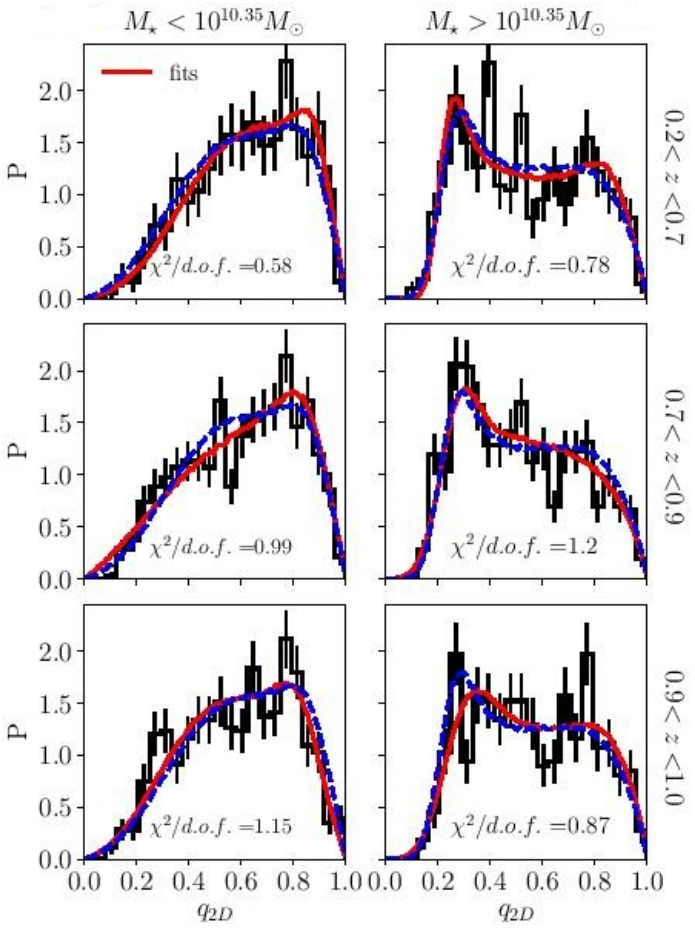

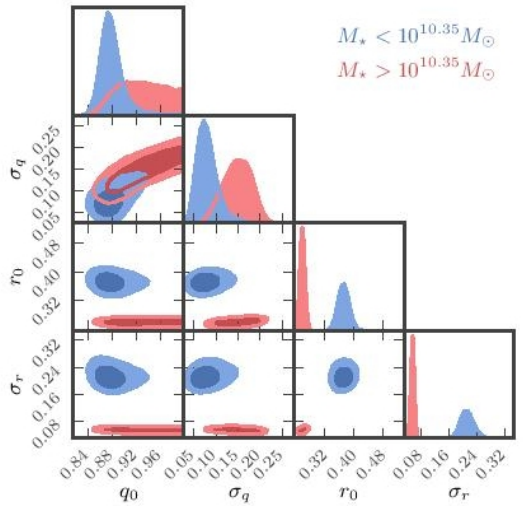

Massive

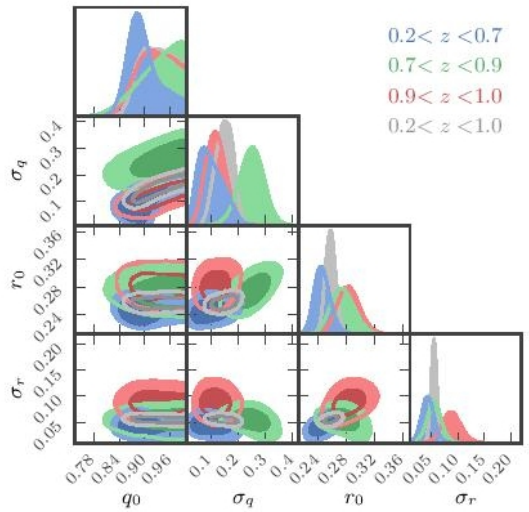

Эволюционирует только радиальный масштаб – у массивных галактик

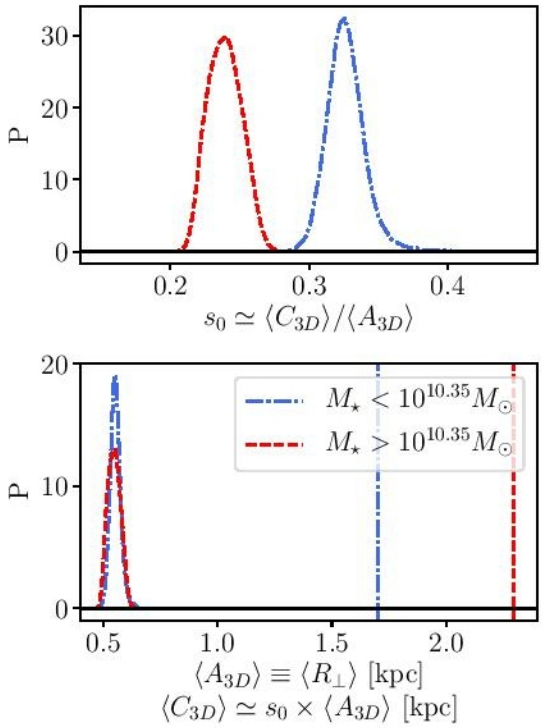

Figure 18. *Top*: MCMC estimate of the marginalized probability distribution for the parameter $s_0 \equiv q_0 r_0$. *Bottom*: Estimate of the probability distribution of the minor axes sizes, assuming that the major axes (marked as horizontal lines) correspond to the comoving effective radius, averaged over all disks with $q_{2D} > 0.5$.

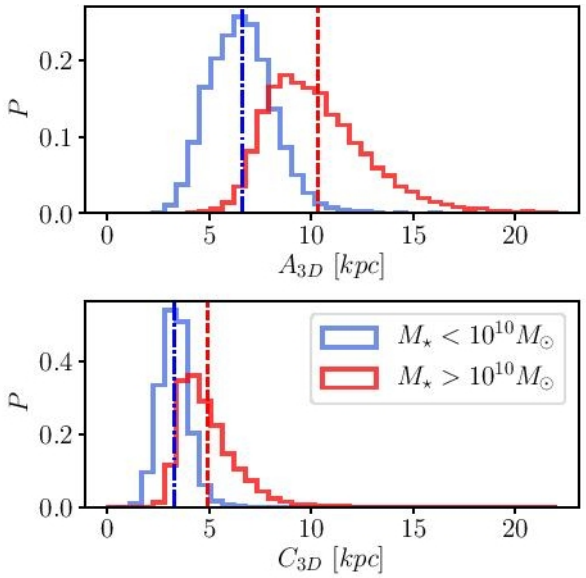

Figure 19. Distribution of minor and major axes sizes, obtained from the simple moment of inertia, for disk galaxies in the HAGN simulation at redshift $z = 1.0$. The axes are re-scaled, such that $(A_{3D} + B_{3D} + C_{3D})/3$ corresponds to the half mass radius. Results are shown for disks with stellar masses higher and lower than $10^{10} M_\odot$, which is slightly above the median stellar mass of 0.74 $10^{10} M_\odot$. Horizontal lines, mark the mean value for each distribution. The figure shows that the absolute sizes of the principle axes increase with mass and that this increase is stronger for the major than for the minor axes, which quantify the disk diameter and thickness respectively.

Толщина дисков не менялась последние 8 млрд лет!

ArXiv: 2010.12586

Tightly coupled morpho-kinematic evolution for massive star-forming and quiescent galaxies across 7 Gyr of cosmic time

Anna de Graaff,[1] Rachel Bezanson,[2] Marijn Franx,[1] Arjen van der Wel,[3,4] Eric F. Bell,[5] Francesco D'Eugenio,[3] Bradford Holden,[6] Michael V. Maseda,[1] Adam Muzzin,[7] Camilla Pacifici,[8] Jesse van de Sande,[9,10] David Sobral,[11] Caroline M.S. Straatman,[3] and Po-Feng Wu[12]

[1] *Leiden Observatory, Leiden University, P.O.Box 9513, NL-2300 AA Leiden, The Netherlands; graaff@strw.leidenuniv.nl*

[2] *Department of Physics and Astronomy, University of Pittsburgh, Pittsburgh, PA 15260, USA*

[3] *Sterrenkundig Observatorium, Universiteit Gent, Krijgslaan 281 S9, B-9000 Gent, Belgium*

[4] *Max-Planck-Institut für Astronomie, Königstuhl 17, D-69117, Heidelberg, Germany*

[5] *Department of Astronomy, University of Michigan, 1085 S. University Avenue, Ann Arbor, MI 48109, USA*

[6] *UCO/Lick Observatory, University of California, Santa Cruz, CA 95064, USA*

[7] *Department of Physics and Astronomy, York University, 4700 Keele St., Toronto, Ontario, M3J 1P3, Canada*

[8] *Space Telescope Science Institute, 3700 San Martin Drive, Baltimore, MD 21218, USA*

[9] *Sydney Institute for Astronomy, School of Physics, A28, The University of Sydney, NSW, 2006, Australia*

[10] *ARC Centre of Excellence for All Sky Astrophysics in 3 Dimensions (ASTRO 3D), Australia*

[11] *Department of Physics, Lancaster University, Lancaster LA1 4YB, UK*

[12] *National Astronomical Observatory of Japan, 2-21-1 Osawa, Mitaka, Tokyo 181-8588, Japan*

ABSTRACT

We use the Fundamental Plane (FP) to measure the redshift evolution of the dynamical mass-to-light ratio ($M_{\rm dyn}/L$) and the dynamical-to-stellar mass ratio ($M_{\rm dyn}/M_*$). Although conventionally used to study the properties of early-type galaxies, we here obtain stellar kinematic measurements from the Large Early Galaxy Astrophysics Census (LEGA-C) Survey for a sample of ~ 1400 massive ($\log(M_*/M_\odot) > 10.5$) galaxies at $0.6 < z < 1.0$ that span a wide range in star formation activity.

Фундаментальная плоскость с пов. яркостью - эволюционирует

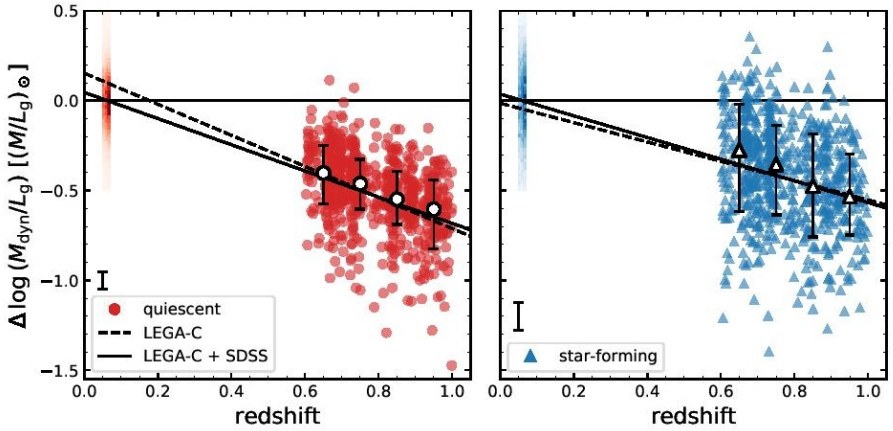

Figure 1. Redshift evolution of the dynamical mass-to-light ratio of quiescent (left) and star-forming (right) galaxies from the SDSS and LEGA-C samples. Linear fits to the LEGA-C data alone (dashed lines) and combined LEGA-C and SDSS sample (solid lines) show that there is a strong evolution in $M_{\rm dyn}/L_g$ with redshift, with the quiescent population evolving more rapidly than the star-forming population (Table 1).

Table 1. Best-fit evolution in $M_{\rm dyn}/L_g$ and $M_{\rm dyn}/M_*$

Sample	$\mathrm{d}\log(M_{\rm dyn}/L_g)/\mathrm{d}z$	$\mathrm{d}\log(M_{\rm dyn}/M_*)/\mathrm{d}z$
$0.6 < z < 1.0$ Q	-0.86 ± 0.07	-0.05 ± 0.06
$0.6 < z < 1.0$ SF	-0.54 ± 0.11	-0.05 ± 0.08
$0.0 < z < 1.0$ Q	-0.728 ± 0.011	0.048 ± 0.009
$0.0 < z < 1.0$ SF	-0.604 ± 0.016	0.097 ± 0.011

NOTE—Samples correspond to either the LEGA-C data ($0.6 < z < 1.0$) or combined SDSS and LEGA-C data ($0.0 < z < 1.0$) for the quiescent (Q) and star-forming (SF) populations.

We assume that the tilt of the FP does not evolve strongly with redshift (as shown in Holden et al. 2010, de Graaff et al. in prep.), and adopt the tilt derived by Hyde & Bernardi (2009), of $a = 1.404$ and $b = -0.761$, for both the SDSS and LEGA-C samples. We fit the zero

We obtain the mass FP by replacing the surface brightness ($I_{\rm e,g}$) by the stellar mass surface density ($\Sigma_* = M_*/(2\pi R_{\rm e}^2)$):

$$\log R_{\rm e} = \alpha \log \sigma + \beta \log \Sigma_* + \gamma, \qquad (6)$$

where α and β describe the tilt, and γ is the zero point. Following the approach of Section 3, we adopt a fixed tilt of $\alpha = 1.629$ and $\beta = -0.84$ (Hyde & Bernardi 2009).

Это и раньше находили

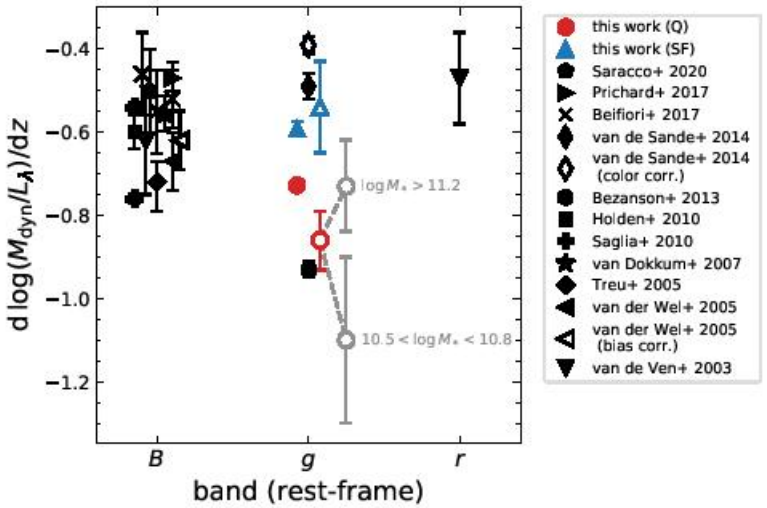

Figure 2. Comparison of the measured redshift evolution in $M_{\rm dyn}/L$ in different passbands. Red and blue markers show the results obtained in this paper for quiescent and star-forming galaxies respectively, for the LEGA-C sample (open) and combined LEGA-C and SDSS sample (solid). Black symbols show results from other studies of quiescent galaxies.

А вот фундаментальная плоскость с пов.плотностью – НЕТ!